



A method for the in-situ determination of the hydraulic conductivity of gravels as used in constructed wetlands for wastewater treatment

P.R. Knowles, P.A. Davies*

Sustainable Environment Research Group, School of Engineering and Applied Science, Aston University, Birmingham, B4 7ET, UK
Tel. +44 (0) 121 204 3724; email: p.a.davies@aston.ac.uk

Received 25 July 2008; Accepted 5 October 2008

ABSTRACT

A new instrument and method are described that allow the hydraulic conductivities of highly permeable porous materials, such as gravels in constructed wetlands, to be determined in the field. The instrument consists of a Mariotte siphon and a submersible permeameter cell with manometer take-off tubes, to recreate *in-situ* the constant head permeameter test typically used with excavated samples. It allows permeability to be measured at different depths and positions over the wetland. Repeatability obtained at fixed positions was good (normalised standard deviation of 1–4%), and results obtained for highly homogenous silica sand compared well when the sand was retested in a lab permeameter (0.32 mm.s^{-1} and 0.31 mm.s^{-1} respectively). Practical results have a $\pm 30\%$ associated degree of uncertainty because of the mixed effect of natural variation in gravel core profiles, and interstitial clogging disruption during insertion of the tube into the gravel. This error is small, however, compared to the orders of magnitude spatial variations detected. The technique was used to survey the hydraulic conductivity profile of two constructed wetlands in the UK, aged 1 and 15 years respectively. Measured values were high (up to 900 mm.s^{-1}) and varied by three orders of magnitude, reflecting the immaturity of the wetland. Detailed profiling of the younger system suggested the existence of preferential flow paths at a depth of 200 mm, corresponding to the transition between more coarse and less coarse gravel layers (6–12 mm and 3–6 mm respectively), and transverse drift towards the outlet.

Keywords: Constructed wetlands; Clogging; Hydraulic conductivity; *In situ*; Measurement

1. Introduction

Over the past two decades Constructed Wetlands (CWs) have become an established technology choice in the UK for the treatment of wastewaters in rural locations. By 2006 it was estimated over 1200 systems existed across the country, predominantly horizontal, sub-surface flow (HSSF) systems used for the tertiary treatment (polishing) of wastewater [1]. In a CW, the wastewater passes below

the surface of a porous gravel bed where the right conditions for final purification are encountered [2]. The hydraulic deterioration of the bed over time as a result of the clogging process can cause short-circuiting and surfacing of the flow [3]. To avoid sub-standard treatment the CW media will eventually require cleaning or replacing — a process which can be very costly.

Exploring the clogging mechanism of the gravel substrate may allow the longevity of the CW to be improved. However, because of the non-cohesive nature of gravel it is difficult to remove integral gravel cores from

*Corresponding author.

the field in a way that allows representative tests to be performed under laboratory conditions [4]. Unfortunately, there is not already a simple technique to measure the permeability of high conductivity materials *in situ* [5], and those that exist for soils are unsuitable. Double ring infiltrometry could be used to determine the ability of the surface to absorb precipitation or surface flow, but would only be effective in CWs with high clogging near the surface [6]. Borehole permeability tests such as the Guelph Permeameter [7] or Amoozemeter [8] techniques allow the conductivity of a vertical soil core to be measured but rely on the soil cohesion and low water table to provide the right test conditions.

The Guelph Permeameter technique has been used to investigate the conductivity of two vertical flow CWs, although the substrates were sand and gravel mixtures with D_{10} (10th percentile diameter) of 0.13 mm and 1.1 mm respectively, and so provided permeabilities within the measuring range of the instrument [9]. However, sandy gravels, as with other fine materials, are unsuitable for use in HSSF CWs because of rapid clogging leading to hydraulic failure [10] — this being the principal reason that European Design Guidelines have steered away from the soil based systems of the original Kickuth Rootzone method and instead recommend gravels with sizes 3–12 mm. These guidelines suggest that once a CW has matured the system will reach an equilibrium hydraulic conductivity of about 1 mm.s^{-1} (86.4 m.d^{-1}) [11]. It has been found that the Guelph Permeameter method is unable to return accurate results for permeability measurements of HSSF CWs which employ these gravels [12]. The objective here is to develop a new method, using broadly similar principles to those mentioned above, but

with improvements making it suitable for measurements with coarse gravel and thus allow the hydraulic conductivities of CWs to be surveyed *in situ*. To allow a full picture of the flow and clogging to be obtained, the method should allow both vertical and horizontal profiling. Further objectives are that instrumentation should be simple to fabricate and use, and that the errors of measurement should be minimised and quantified.

2. Experimental method

2.1. Theory

The method is a combination of two main principles applied *in situ*: the Mariotte Siphon principle, used to create a small, constant head in an open tank of water, thus controlling the discharge from it, and the constant head permeability test [13]. From this point on, all letters in square brackets refer to those labels indicated on Fig. 1. As shown in Fig. 1, a PVC tube with diameter at least equal to ten times the largest gravel particle diameter is driven vertically into the bed. This constitutes the permeameter cell [h], entrapping a gravel core [p,r] with length L_{CELL} and cross-sectional area A_{CELL} .

During the test, the water level in the tube is brought to above the gravel surface and kept constant by using the Mariotte Siphon technique. This is achieved by using a reservoir device [g], similar to the Guelph Permeameter [14], but enlarged to make it suitable for applications in higher conductivity media such as gravel ($1000 > k > 1 \text{ mm.s}^{-1}$) as well as the lower conductivity porous media for which the Guelph Permeameter is intended.

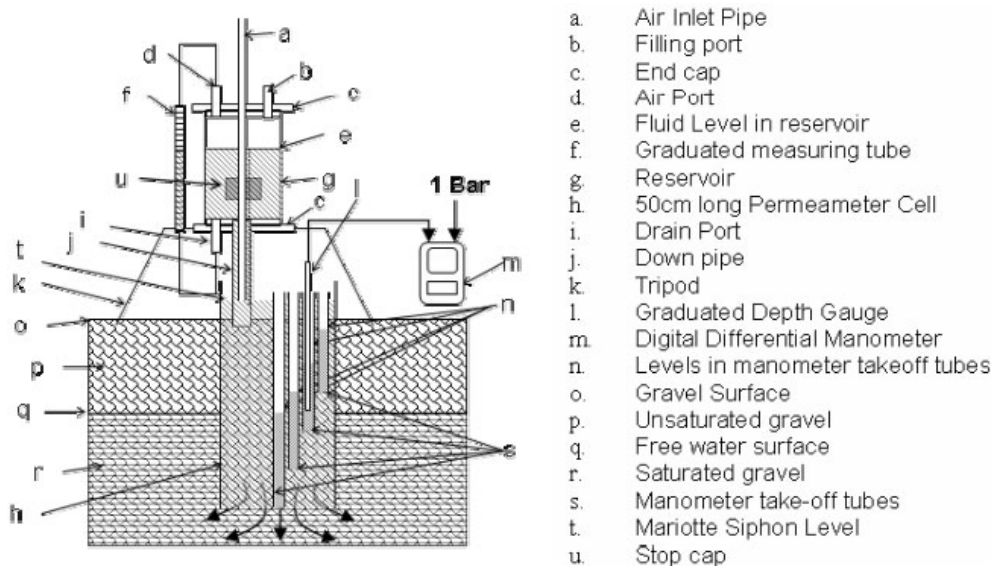


Fig. 1. Experimental set-up for in-situ determination of the hydraulic conductivity of highly porous media (not to scale: reservoir stands approx. 1 m off the ground).

Four manometer take-off tubes [s], ranging from 200 to 500 mm length in 100 mm increments, are inserted into the gravel core prior to the experiment commencing, to provide n (in this case 4) evenly distributed take-off points at 100, 200, 300 and 400 mm depths into the gravel core. Using a digital differential manometer [m] with a 500 mm graduated depth gauge [l] it is possible to determine the static [q] and dynamic [n] water levels in each take-off tube, thus allowing the vertical head loss across each 100 mm section (h_n) to be measured. By monitoring the discharge of water (q') from the reservoir [e,f], in keeping the permeameter head (h_T) constant, it is possible to calculate the permeability of the gravel core (k_T) using Darcy's Law [Eq. (1)]. Subsequently the permeability of each 100 mm section (k_n) can be found [Eq. (2)]. The test provides vertical conductivity profiles, although by interpolating between sample points it would be possible to predict a horizontal conductivity profile. This is based on the assumption that flow would behave identically in both planes. It is worth mentioning that the head is applied across a layer of gravel media which was previously unsaturated. It is assumed that upon commencing the experiment this layer become suitably saturated so that Darcy's Law, and not Richard's Law, is the governing equation for flow. If only the permeability of the wetted gravel is of interest, the unsaturated layer should be removed from the permeameter cell before commencing the experiment, and the subsequent analysis modified to reflect the new test conditions.

$$k_T = \frac{q \times L_{CELL}}{A_{CELL} \times h_T} \quad (1)$$

$$k_n = \frac{1}{n \left(\frac{h_n}{h_T \cdot k_T} \right)} \quad (2)$$

Fig. 2 illustrates how the dynamic levels in each take-off tube might be expected to vary because of the head loss down the length of the permeameter cell. Fig. 2 also gives a more detailed appreciation of how Darcy's Law can be applied to the experimental setup, using the electrical analogy of a wire of constant dimensions but varying electrical resistivity, being split into n equally lengthened sections which represent different resistances in series. In Fig. 2 the reciprocal of electrical resistivity is used — electrical conductivity.

2.2. Apparatus

Fig. 3 depicts the apparatus during an experiment at a CW, whilst Fig. 4 shows the apparatus laid out so that the

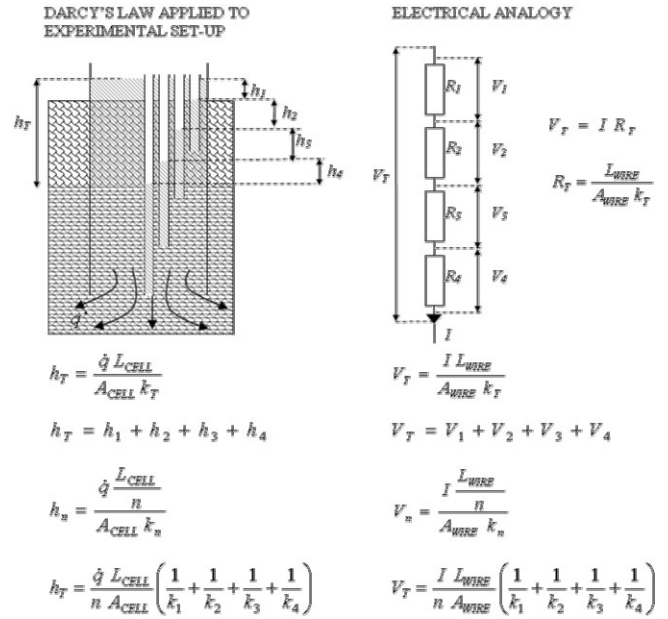


Fig. 2. A more detailed consideration of the theory underlying the experimental method, with an electrical analogy — the voltage drop across a wire of constant dimensions but variable electrical conductivity, split into lengths of equal section.



Fig. 3. Photograph of the experimental set-up at a Constructed Wetland in South Warwickshire, UK, depicting the Mariotte Siphon activated reservoir standing above the permeameter cell, which has been submersed into the gravel substrate.

actual components can be seen. The corresponding list of components used to assemble the Mariotte siphon activated reservoir, and other apparatus used in the experiment, is provided in Table 1 with costings and supplier information. Total cost for all equipment was £1055 although almost 90% of this was apportioned to the purchase of the four digital manometers used in the experiment.

Table 1

List of the major components used to make the apparatus for the experiment. Costs are rounded to the nearest pound sterling and reflect 2008 UK prices. Only the components which are considered specialist or difficult to identify are listed. As indicated, some components were manufactured or modified in house to make them appropriate for the apparatus. Components which are considered widely available do not have a specific supplier listing.

Label	Part	Product	Supplier	Cost (£)
a,s	Air inlet pipe, manometer take-off tubes	15 mm diameter speedfit barrier pipe	John Guest, Middlesex, UK	2
b,d,i	Filling port, air port, drain port	15 mm speedfit tank connector	John Guest, Middlesex, UK	4
c	End caps	Aluminium plate	N/A Manufactured in house	25
f	Graduated measuring tube	25 ml acrylic burette tube	Scilabware, Staffs., UK	22
g	Reservoir chamber	L0.33 m D0.2 m, wall 0.003 m polycarbonate tube	Wake Plastics, Middlesex, UK	50
h	Permeameter cell	L0.5m D0.168m wall 0.004m PVC ducting	N/A modified in house	4
j	Down tube	1" PVC tank connector with 1.5" PVC plain socket adaptor and 1.5" PVC pipe	George Fischer, Coventry, UK	20
k	Tripod legs	3* floor tom drum legs	N/A	20
l	Graduated depth probe	6 mm OD 1.5 mm wall acrylic tube	N/A modified in house	5
m	Digital Manometers	1 * Digitron 2080P	Sifam, Devon, UK	300
m	Digital Manometers	3 * Kane 3100-1	Kane International, Herts., UK	600
u	Stop cap	Rubber plunger head	N/A	1
v	T-Bar	1.25" PVC pipe	N/A	1
w	Metal stakes	10 mm OD CSS steel tube	N/A Manufactured in house	1
Total cost				1055

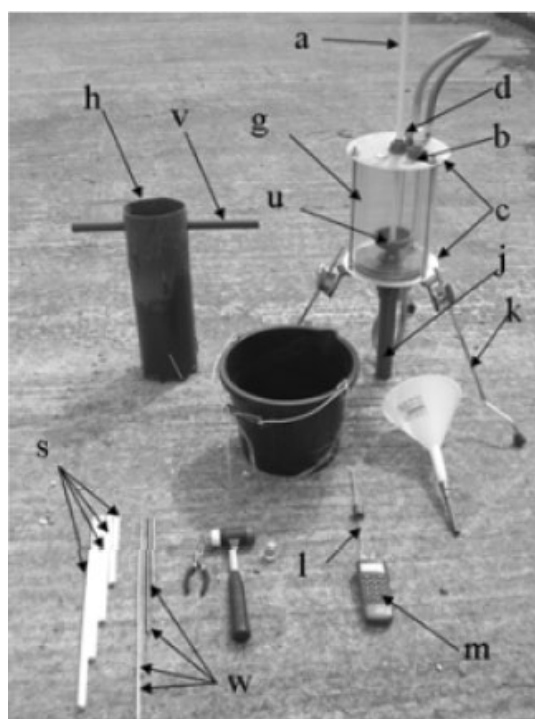


Fig. 4. Photograph of the full inventory of apparatus used in the experiment (labels as per Fig. 1). The method is designed to be highly portable so that it can be performed by one user, in-situ. a. air inlet pipe, b. filling port, c. end cap, d. air port, g. reservoir, h. 50 cm long Permeameter cell, j. down pipe, k. tripod, l. graduated depth gauge, m. digital differential manometer, s. manometer take-off tubes, u. stop cap, v. T-bar accessory, w. metal stakes.

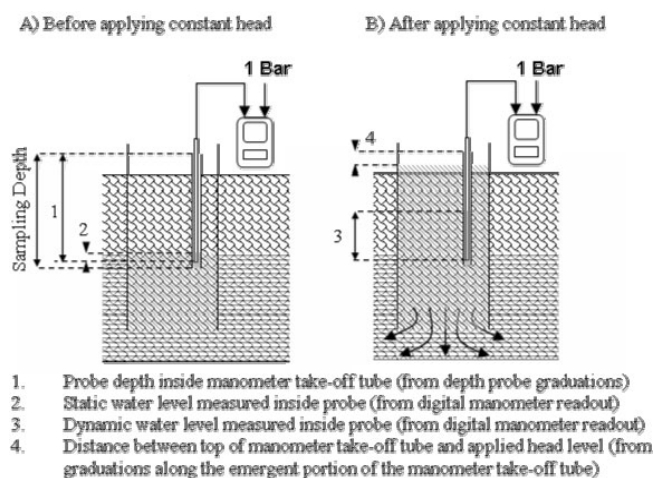


Fig. 5. Measurements that are taken during the experiment, depicted for one take-off tube. Corresponding readings will need to be taken in each individual take-off tube. N.B. For clarity, the reservoir device which maintains the constant head has been omitted from graphic B): "After applying constant head".

2.3. Experimental procedure

The instructions followed when performing the experiment are listed below where the labels in square brackets refer to the components illustrated in Figs. 1 and 4. To aid clarity, Fig. 5 illustrates how some of the measurements described in the subsequent procedure are obtained.

1. Drive the permeameter cell [h] into the gravel until the top 100 mm is emergent from the gravel surface, thus creating a 400 mm gravel plug. Serrations are cut into the penetrating end of the permeameter cell to aid its insertion into the gravel, and there are two holes at the top of the tube to allow a T-Bar accessory [v] to be utilized. To minimise disturbance to the gravel core, a circular jigsaw cutting action should be used to submerge the tube into the gravel.

2. Insert the four manometer take-off tubes [s] to the required depths, so that the top of them is in line with the top of the permeameter cell. To aid insertion of the take-off tubes four metal stakes [w] with lengths just greater than, and ODs just smaller than, the respective dimensions of the take-off tubes, can first be driven into the ground. The take-off tube is then sheathed over the top of the stake and driven into the gravel until the stake re-emerges from the top of the take-off tube. Once the stake has been removed, the inside of the take-off tube is left free from gravel blockages. This ensures the water level inside the take-off tube is free to fluctuate only according to the hydraulic conditions in the permeameter cell; this otherwise being a possible source of error in measurements.

3. Attach a graduated depth probe [l] to each manometer [m] and insert one probe into each take-off tube to locate the static water level. The distance the probe is immersed into the water should be small, to minimise errors caused by displacement. Record the digital manometer readings after they have stabilised, and the distance the probes have been inserted into the take-off tube. This may not be possible in all the tubes depending on the water level in the bed, but as a check, any readings obtained should be roughly equal. Any disparity between the readings will be caused by minor differences between the vertical alignments of the top of the take-off tubes, and therefore, recording the different static water level readings will allow these discrepancies to be accounted for.

4. Assemble the Mariotte siphon activated reservoir by combining the parts as illustrated in Figures 1–4. Adjust the tripod legs [k] so that the down pipe [j] rests just above the surface of the gravel. Lower the air pipe [a] so that it is in line with the end of the down pipe and so the stop cap [u] inside the reservoir covers the down pipe inlet.

5. Open the filling [b] and air ports [d] on the reservoir and fill the reservoir with water. This is done using a bucket and long stem funnel although any method is applicable. Close the air and filling ports.

6. Pre fill the permeameter cell [h] with water until the water level rises to just above the gravel surface. This will maximise the amount of water inside the reservoir that can be used for steady measurements.

7. Raise the air pipe [a] so that the water level in the cell settles at a height above the gravel surface, but below the lip of the cell. The Mariotte Siphon will engage and the reservoir will begin to empty to maintain the constant head inside the cell. Measure the water level indicated by the graduated measuring tube [f] and begin timing. The emergent 100 mm of the take-off tubes have a scale marked on them so that the distance between the top of the take-off tubes and the water level inside the permeameter cell can be accurately recorded. This allows the total applied head across the permeameter cell, and corresponding head loss measured in each take-off tube, to be accurately calculated.

8. The value indicated by the manometers will change to reflect the dynamic water level inside the take-off tubes. Record the digital manometer readings after they have stabilised. This stage must be completed before the reservoir empties.

9. Record the water level in the graduated measuring tube against time.

2.4. Accuracy

Experimental accuracy was tested by measuring the hydraulic conductivity of fine silica sand using both a laboratory standard constant head permeameter (ELE, Bedfordshire) and the proposed method. Hydraulic conductivity values of 0.323 mm.s^{-1} and 0.314 mm.s^{-1} were obtained for the standard and proposed method respectively. These values are within the range often quoted in the literature for the permeability of silica sand; 0.1 mm.s^{-1} to 1 mm.s^{-1} [15–17]. Fig. 6 shows the hydraulic head loss over the sand plug used in each experiment, as obtained using manometer take-off points. Silica sand is very homogeneous and so the hydraulic gradient should be linear; which was achieved with both the standard and proposed methods, returning R^2 fits of 0.990 and 0.999 respectively.

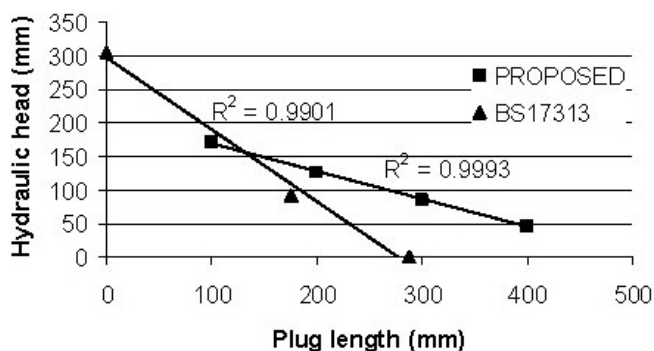


Fig. 6. Head loss across homogeneous silica sand cores, tested using both BS17313 and the proposed method. Good linearity was achieved in both cases.

2.5. Repeatability

An experiment was performed *in-situ* at a tertiary wastewater treatment CW in Fenny Compton, UK (Severn Trent Water Plc.). The gravel media had a size distribution between 6 mm and 12 mm diameter. The permeameter cell was immersed at a point near the CW inlet and the experiment repeated five times to ensure the repeatability of the method. This is seen to be good in Fig. 7, with standard deviations ranging from 1% to 4% of total normalised head loss, between 100 mm and 400 mm depth respectively. As evident from Fig. 7 the small fractional head loss which remains at a 400 mm depth indicates that exit losses from gravel cores to the CW macrocosm are usually negligible.

Another repeatability experiment was performed *in-situ* at a tertiary wastewater treatment CW in Moreton Morrell, UK (Severn Trent Water Plc.), under wet weather conditions. The gravel size distribution varied between 3 mm and 9 mm diameter. The addition of precipitation created unsteady test conditions, affecting the static and dynamic water levels measured in each take-off tube between experimental runs. Fig. 8 shows that standard deviations ranged from 6% to 18% of the total normalised head loss. Resultantly, it is recommended that either the

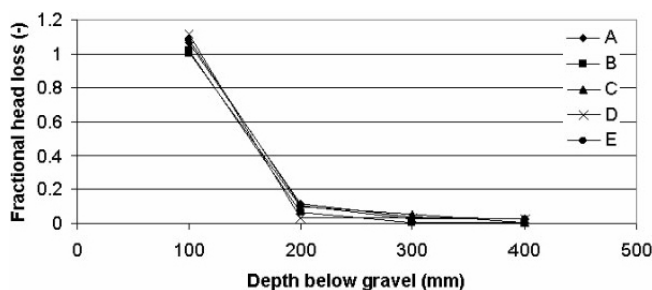


Fig. 7. Head loss across a gravel core in a CW in Fenny Compton, UK. The test was repeated five times (Runs A–E) to determine that the experimental repeatability was good; returning standard deviations of 1–4% of total normalised head loss.

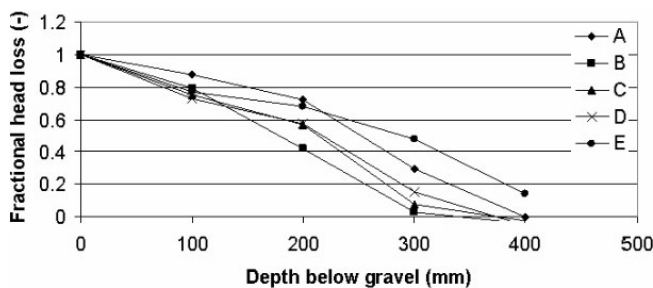


Fig. 8. Head loss across a gravel core in a CW in Moreton Morrell, UK. The experiment was conducted under precipitation conditions which adversely affected repeatability; returning standard deviations of 6–18% of total normalised head loss.

experimental method only be performed under dry weather conditions, or the orifice of the permeameter cell be sufficiently covered to avoid precipitation gains.

2.6. Sources of error

The most common sources of error when performing the experiment, and methods for minimising them, are detailed in Table 2. Fig. 9 shows the results of Run A of the Moreton Morrell repeatability experiment, with associated maximum and minimum errors. Fig. 9a includes the +20% of manometer readout error, associated with the displacement caused by depth probe insertion, whereas Fig. 9b omits this. It can be seen that taking the instantaneous reading off the manometer, and reinserting the

Table 2

Errors associated with the experiment and ways of minimising them

Error	Magnitude	Minimisation
Use of digital manometer	±0.15% reading ±0.15% fixed error ±0.2% display resolution	Unavoidable
Insertion of depth probe causing displacement	+20% of actual reading ±1 mm	Allow time for reading to stabilize
Misreading reservoir level	±1 mm	Use graduated scale
Stop watch error	±0.5 s	Use large reservoir volume

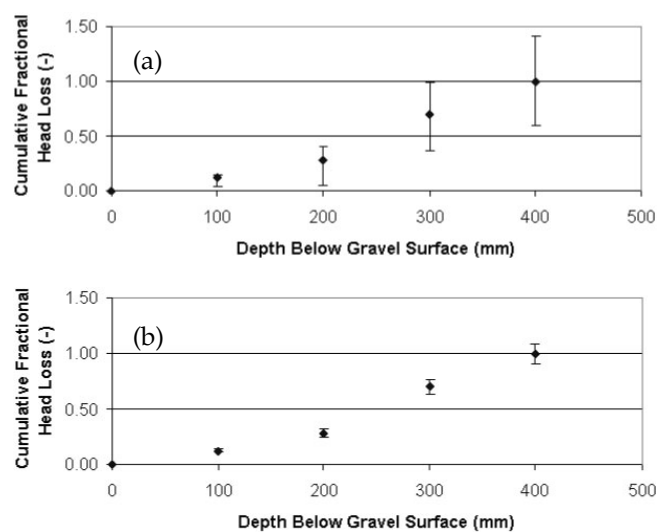


Fig. 9. Errors associated with the results of Run A of the Moreton Morrell repeatability experiment, both with (a) and without (b) inclusion of the error introduced by instantaneous reading of the manometer, and reinsertion of the probe between readings.

probe between static and dynamic readings, increases the associated error, for example, with the 400 mm depth measurement, from $\pm 9\%$ to $\pm 40\%$ of the total normalised head. Therefore, it should be ensured that the initial static reading is allowed to stabilise before being recorded, and that a different manometer is used with each take-off tube to negate the requirement to reinsert the probe between static and dynamic level readings.

One major source of error which does not appear in Table 2 because it is difficult to quantify, is the effect of inserting the permeameter cell into the media. Accumulated solids are 99% interstitial [18], and their deposition through precipitation as gelatinous black sludges or bonding by biomass secretions is thought to be one of the major mechanisms of CW clogging [19,20]. Forcing the permeameter cell into the gravel requires mechanical agitation of the sample and may cause compaction, destroy bonds between interstitial solids and will consequently have an adverse affect on the representativeness of results. Regarding compaction, it should be ensured that after insertion of the permeameter cell the sample level on the inside of the tube is at a similar level to the substrate on the outside of the tube. Any discrepancy between these two levels suggests that sample compaction has occurred and the experiment would be better conducted at a new point close by. Even after observing this recommendation, there is the possibility that variable degrees of sample disturbance would be caused, thus affecting the validity of the results. To try and ascertain the extent of the possible variance, so that a level of accuracy for the experiment could be quoted, an investigation was conducted whereby the experiment was repeated at several points in close proximity. The assumption is that the hydraulic conditions between these points would be fairly homogeneous, and as such the method would return similar results. Small differences in hydraulic conductivity will naturally arise between proximal cores because of slight heterogeneity between particle size distributions and varying root densities [21], but it is expected that results would be within an order of magnitude.

Fig. 10 shows the location of the sampling points for the homogeneity experiment, which was performed at the Moreton Morrell CW. Four points were chosen (A1, B2, C3 and D4) and matrices of three additional sampling points were closely installed around each of these points. The range of cumulative hydraulic conductivity values for the four groups of holes, along with averages and standard deviations are reported in Table 3. Hydraulic conductivity is 3 orders of magnitude lower at the inlet ($10^{-2} \text{ mm.s}^{-1}$) than elsewhere (10^1 mm.s^{-1}) due to solids accumulation in this region, and generally increases with distance from the inlet, as has been observed in other studies [22]. Regarding variance in each group of holes, standard

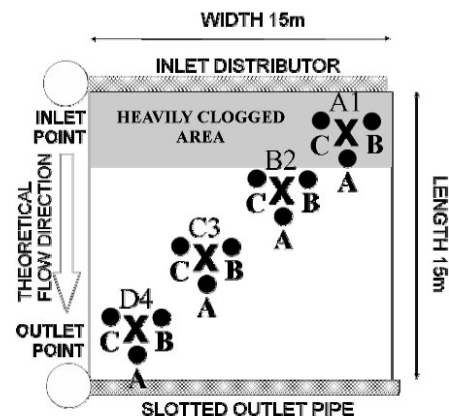


Fig. 10. Locations of 16 sampling points installed to perform a homogeneity experiment at Moreton Morrell CW, to assess the possible errors introduced by inserting the permeameter cell into the gravel (not to scale: points marked X were set at a vertical and horizontal pitch of 4 m. Points marked • were arranged around the X points at a 0.2 m radius).

Table 3

Range of hydraulic conductivity values, averages and standard deviations recorded for each group of holes during the homogeneity experiment

Group	Hydraulic conductivity, mm.s^{-1}			
	Max.	Min.	Avg.	St. Dev.
A1	0.10	0.01	0.04	0.02
B2	3.98	2.09	3.02	0.83
C3	3.50	2.72	3.31	0.39
D4	14.25	4.62	9.28	3.41

deviation is always within the order of magnitude of the average hydraulic conductivity. Additionally, apart from near the inlet region where very small differences between results appear relatively large when compared to the low conductivity values measured, the standard deviation was always within 30% of the average. It can therefore be stated that, when applied *in situ*, the method returns results representative of the order of magnitude of the hydraulic conductivity of the substrate in that area, and the practical reading recorded has a $\pm 30\%$ associated degree of uncertainty because of the mixed effect of localised differences in gravel core profiles and sample disturbance during insertion of the tube into the gravel.

2.7. Data analysis

The field results and subsequent processes to calculate the conductivity information required for Run A of the Moreton Morrell repeatability experiment are given as an example in Table 4. The number labels for the readings obtained from the probe (1–4) correspond to those measurements labelled in Fig. 5.

Table 4

Example of the readings recorded and subsequent calculation steps. Steps 1–4 refer to readings taken from the probe and correspond to those measurements illustrated in Fig. 5

Test Moreton Morrell repeatability test Run A							
Readings from Mariotte Siphon activated reservoir							
Reservoir level at t_0	mm	55			Cell length	mm	400
Reservoir level at t_n	mm	170			Cell diameter	mm	168
Change	mm	115					
Reservoir diameter	mm	194					
Volume passing	m ³	0.0034					
Time elapsed	s	76					
Readings from probe (see Fig. 5)							
Sampling depth	mm	400	300	200	100	Step	
Probe depth in takeoff tube	mm	300	300	250	150	1	
Static water level	mm	34	26	N/A	N/A	2	
Dynamic water level	mm	30	95	138	78	3	
Head level below take-off	mm	50	50	50	45	4	
Total head	mm	216	224			5	=1-2-4
Average total head	mm	220				6	
Core conductivity	m.d ⁻¹	323				7	Eq. (1)
Vertical conductivity profile calculations							
Vertical section	mm	300–400	200–300	100–200	0–100		
Cumulative head loss	mm	220	155	62	27	8	= 1-3-4
Sectional head loss	mm	65	93	35	27	9	= 8-8 ^a
Fractional head loss		0.30	0.42	0.16	0.12	10	= 9/6
Cumulative fract. head loss		1.00	0.70	0.28	0.12	11	= 10 ^a + 10
Apportioned conductivity	m.d ⁻¹	273	191	507	658	12	Eq. (2)

^aIndicates the same parameter, but that of the proceeding vertical section.

3. Application example

The test was used to profile the permeability of the entire CW at Fenny Compton which measures 12 m L, 40 m W, and 0.6 m H, where the flow moves along the longitudinal axis from inlet to outlet. A 4×5 matrix of sampling points was arranged with locations indicated on Fig. 11 and the test conducted in January 2008. The results for the five transverse sections P1–P5 are shown in Fig. 12.

The darker areas in Figs. 11 and 12 represent those areas which are more clogged and have a lower hydraulic conductivity. It is probable that these regions correspond to the preferential flow regimes that have previously existed within the CW, because high flows brings greater solids loading, increasing the rate of clogging [23]. Hydraulic conductivities at specific points ranged from 0 mm.s⁻¹ up to 913 mm.s⁻¹, although most values were below 100 mm.s⁻¹, so the scale in Fig. 12 is capped at 100 mm.s⁻¹ to aid visual contrast. The experiments at Fenny Compton were conducted approximately 1 year after the bed was refurbished, so the relatively high conductivity values measured reflect the young state of the bed.

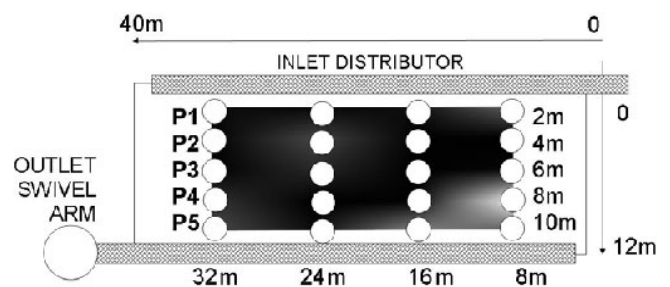


Fig. 11. Plan view of Fenny Compton CW showing location of sampling points (not to scale).

Generally, the hydraulic conductivity in the bed increases with distance from the inlet, as suggested by the increasing ratio of light to dark areas in each successive cross section of Fig. 12. Low values at section 1 purport to high solids accumulation near the inlet. The visualizations suggest a preferential flow path between 200 mm and 300 mm below the gravel surface, which shifts towards the outlet swivel arm with distance from the inlet as a result of potential flow [24]. Many occurrences of preferential bottom flow have been reported in the literature so it was

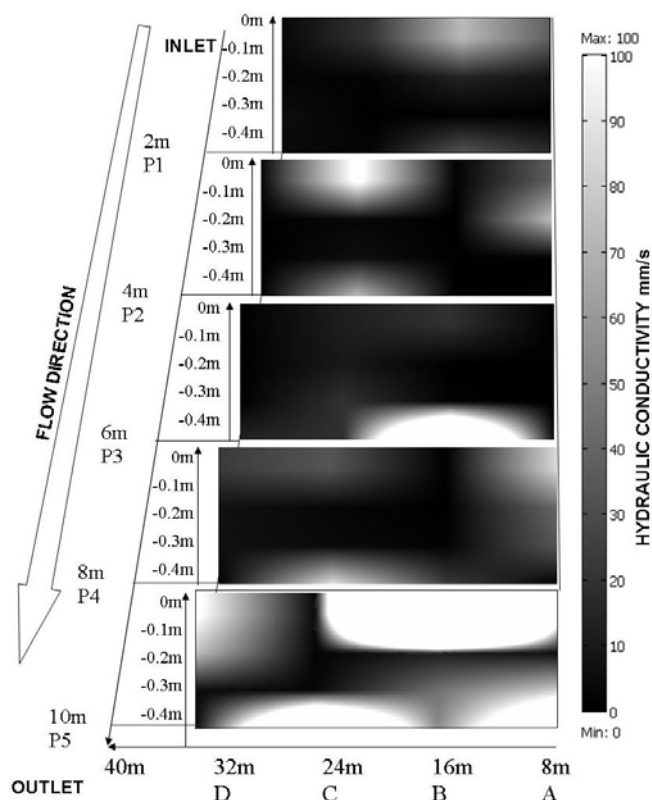


Fig. 12. Calculated permeability profiles for five transverse sections at Fenny Compton (not to scale). Darker regions represent areas of lower hydraulic conductivity and therefore greater clogging. The scale has been capped at 100 mm.s^{-1} to aid visual contrast.

expected that the most clogged areas would be found between the 300 mm and 400 mm depth [25–27]. However, upon excavating the gravel cores for analysis, it was found that two different grades of gravel constituted the substrate profile; 3–6 mm diameter gravel between 200 mm and 400 mm depth, and 6–12 mm diameter gravel in the top 200 mm. Preferential flow may therefore occur along the bottom of the coarser strata given the favourable hydraulic conditions [28].

4. Conclusions

The instrument developed for *in situ* permeability measurement in constructed wetlands is suitable for measurement of permeabilities up to the order of $O(10^3 \text{ mm.s}^{-1})$ approximately corresponding to gravel sizes up to 15 mm diameter. In the version described here, it is used to characterise four adjacent sections of gravel core each of diameter 160 mm and height 100 mm, at progressively increasing depths from the surface. (However, the design could readily be adapted for different sizes of core). Since the instrument is made mainly from standard plastic tubes and parts produced in an engineer-

ing workshop, it is straightforward to replicate and fabricate. Detailed instructions for its use, and the interpretation of the readings based on Darcy's law, have been given. The instrument weighs about 3 kg, making it portable, and costs about £150 to build. The four digital manometers used in the experiment cost between £200 and £300 each bringing the total cost to £1055. Depending on the permeability, a set of readings covering the four depths takes about 20 min, including sample preparation. It has been tested at two CW sites in Warwickshire, UK.

Although the repeatability of the instrument at a given location is 1–4%, practical accuracy is about 30% and this is probably due to disruption in the gravel core on insertion of the instrument, and to inherent local heterogeneity of the gravel and rhizosphere. Work is in progress to elucidate further the cause of this error, although the error is relatively small considering that over the bed, permeability variations of 4 orders of magnitudes occur.

Based on these pilot results, it will now be possible to survey a range of other CWs. The planned experiments will be complemented by dye tracing experiments and mathematical modelling to reveal whether the preferential flow paths that exist correspond to the state of clogging. Using these methods it is expected to identify the major factors which cause premature hydraulic failure of HSSF CWs.

Acknowledgements

This work was made possible thanks to joint funding from Severn Trent Water Plc. (UK) and a CASE studentship granted by the EPSRC UK (ref. CASE/CNA/06/28). The authors wish to thank Dr. Paul Griffin of Severn Trent Water for his collaboration.

References

- [1] P. Cooper, The Constructed Wetland Association UK database of constructed wetland systems. *Water Sci. Technol.*, 56 (2007) 1–6.
- [2] International Association on Water, Constructed wetlands for pollution control: processes, performance, design and operation. IWA Publishing, London, UK, 2000.
- [3] D. Cooper, P. Griffin and P. Cooper, Factors affecting the longevity of sub-surface horizontal flow systems operating as tertiary treatment for sewage effluent: Part 2, in 10th International Conference on Wetland Systems for Water Pollution Control. Lisbon, Portugal, 2006.
- [4] E. Ranieri, Hydraulics of sub-superficial flow constructed wetlands in semi-arid climate conditions. *Water Sci. Technol.*, 47(7–8) (2003) 49–55.
- [5] R.H. Kadlec and R.L. Knight, *Treatment Wetlands*, Boca Raton, Florida, 1996.
- [6] ASTM-D3385, Standard Test Method for Infiltration Rate of Soils in Field Using Double-Ring Infiltrometer, American Society for the Testing of Materials, 2003.
- [7] ASTM-D5126, Standard Guide for Comparison of Field Methods for Determining Hydraulic Conductivity in the Vadose Zone, American Society for the Testing of Materials, 2004.

- [8] A. Amoozegar, A compact constant-head permeameter for measuring saturated hydraulic conductivity of the vadose zone. *Soil Sci. Soc. Amer. J.*, 53(5) (1989) 1356–1361.
- [9] G. Langergraber, R. Haberl, J. Laber and A. Pressl, Evaluation of substrate clogging processes in vertical flow constructed wetlands. *Water Sci. Technol.*, 48(5) (2003) 25–34.
- [10] W.E. Sanford, T.S. Steenhuis, J.Y. Parlange, J.M. Surface and J.H. Peverly, Hydraulic conductivity of gravel and sand as substrates in rock-reed filters. *Ecol. Eng.*, 4(4) (1995) 321–326.
- [11] P.F. Cooper, G.D. Job and M.B. Green, Reed beds and constructed wetlands for wastewater treatment. Water Research Centre, WRC Publications, Medenham, Marlow, Buckinghamshire, UK, 1996.
- [12] M. Mastrorilli, E. Ranieri and V. Simeone, Evaluation of hydraulic conductivity in a phragmites wastewater treatment plant, in: *Progress in Water Resources*, Rhodes, Greece, 2001.
- [13] BS-ISO-17313, Soil quality. Determination of hydraulic conductivity of saturated porous materials using a flexible wall permeameter. British Standards Institute, UK, 2004.
- [14] W.D. Reynolds and D.E. Elrick, A method for simultaneous in situ measurement in the vadose zone of field-saturated hydraulic conductivity, sorptivity and the conductivity-pressure head relationship. *Ground Water Monitor. Rev.*, 6(1) (1986) 84–95.
- [15] E. Smith, R. Gordon, A. Madani and G. Stratton, Cold climate hydrological flow characteristics of constructed wetlands. *Canadian Biosystems Engineering / Le Genie des biosystems au Canada*, 2005.
- [16] R.F. Craig, *Craig's Soil Mechanics*, 7th ed., Taylor & Francis, Abingdon, UK, 2004, p. vii, 447.
- [17] G.E. Barnes, *Soil Mechanics: Principles and Practice*, 2nd ed., Macmillan, Basingstoke, UK, 2000, p. xviii, 493.
- [18] A. Caselles-Osorio, J. Puigagut, E. Segu, N. Vaello, F. Granés, D. García and J. García, Solids accumulation in six full-scale subsurface flow constructed wetlands. *Water Res.*, 41(6) (2007) 1388–1398.
- [19] C. Platzer and K. Mauch, Soil clogging in vertical flow reed beds — Mechanisms, parameters, consequences and solutions? *Water Sci. Technol.*, 35(5) (1997) 175–181.
- [20] R. Blazejewski and S. Murat-Blazejewska, Soil clogging phenomena in constructed wetlands with subsurface flow. *Water Sci. Technol.*, 35(5) (1997) 183–188.
- [21] H.J. Bavor and T.J. Schulz, Sustainable suspended solids and nutrient removal in large-scale, solid matrix, constructed wetlands systems, in: *Constructed Wetlands for Water Quality Improvement: Conference, Selected papers*, G.A.E. Moshiri, ed., Lewis, Boca Raton, FL, 1993, pp. 219–225.
- [22] R.H. Kadlec and J.T. Watson, Hydraulics and solids accumulation in a gravel bed treatment wetland, in: *Constructed Wetlands for Water Quality Improvement: Conference, Selected papers*, G.A.E. Moshiri, ed., Lewis, Boca Raton, FL, 1993, pp. 227–235.
- [23] C.C. Tanner, J.P.S. Sukias and M.P. Upsdell, Organic matter accumulation during maturation of gravel-bed constructed wetlands treating farm dairy wastewaters. *Water Res.*, 32(10) (1998) 3046–3054.
- [24] J. García, E. Ojeda, E. Sales, F. Chico, T. Píriz, P. Aguirre and R. Mujeriego, Spatial variations of temperature, redox potential, and contaminants in horizontal flow reed beds. *Ecol. Eng.*, 21(2–3) (2003) 129–142.
- [25] M.T. Waters, D.H. Pilgrim, T.J. Schulz and I.D. Pilgrim, Variability of hydraulic response of constructed wetlands, in: *Proc., National Conference on Hydraulic Engineering*, 1993.
- [26] P.J. Fisher, Hydraulic characteristics of constructed wetlands at Richmond, NSW, Australia. *Constructed Wetlands in Water Pollution Control*, 1990, pp. 21–31.
- [27] J.K. Rash and S.K. Liehr, Flow pattern analysis of constructed wetlands treating landfill leachate. *Water Sci. Technol.*, 40(3) (1999) 309–315.
- [28] F. Suliman, C. Futsaether and U. Oxaal, Hydraulic performance of horizontal subsurface flow constructed wetlands for different strategies of filling the filter medium into the filter basin. *Ecol. Eng.*, 29(1) (2007) 45–55.